Improved groundwater representation at regional scale — coupling of mesoscale Hydrologic Model (mHM v5.7) with OpenGeoSys (OGS)

Miao Jing[1], Falk Heße[1], Rohini Kumar[1], Wenqing Wang[2], Thomas Fischer[2], Marc Walther[2,3], Matthias Zink[1], Alraune Zech[1], Luis Samaniego[1], Olaf Kolditz[2,4], and Sabine Attinger[1,5]

[1]Department of Computational Hydrosystems, UFZ – Helmholtz Centre for Environmental Research, Permoserstr. 15, 04318 Leipzig, Germany
[2]Department of Environmental Informatics, UFZ – Helmholtz Centre for Environmental Research, Permoserstr. 15, 04318 Leipzig, Germany
[3]Institute of Groundwater Management, Technische Universität Dresden, Bergstr. 66, 01069 Dresden, Germany
[4]Applied Environmental Systems Analysis, Technische Universität Dresden, Dresden, Germany
[5]Institute of Earth and Environmental Sciences, University of Potsdam, Karl-Liebknecht-Str. 24–25, 14476 Potsdam, Germany

Correspondence to: Miao Jing (miao.jing@ufz.de)

Abstract.

Most large-scale hydrologic models fall short in reproducing groundwater head dynamics due to their over-simplified representation of groundwater flow. In this study, we aim to extend the applicability of the Mesoscale Hydrologic Model (mHM v5.7) to subsurface hydrology through the coupling with simulator OpenGeoSys (OGS). The two models are one-way coupled through a model interface GIS2FEM, by which grid-based fluxes generated by mHM are converted into upper surface boundary conditions of the groundwater model OGS. Specifically, the grid-based vertical reservoirs in mHM are completely preserved for land-surface fluxes, while OGS acts as a plug-in to the original mHM modeling framework for groundwater flow and transport modeling. The applicability of the coupled model (mHM#OGS v1.0) is evaluated by a case study in central European meso-scale river basin Nägelstedt. Different time steps, daily in mHM and monthly in OGS, are used to account for fast surface flow and slow groundwater flow. Model calibration is conducted following a two-step procedure using discharge and long-term mean of groundwater head measurements, respectively. Based on the model summary statistics, Nash–Sutcliffe model efficiency (NSE), Pearson correlation R_{cor}, and inter-quantile range error QRE, the coupled model is able to satisfactorily represent the dynamics of discharge and groundwater heads at several locations across the study basin. Our exemplary calculations show that the coupled model can take advantage of the spatially explicit modeling capabilities of surface and groundwater hydrologic models, and provide us with adequate representation of the spatio-temporal behaviors of groundwater storages and heads, thus making it valuable tool for addressing water resources and management problems.

1 Introduction

Historically, large-scale hydrologic models are commonly developed to predict discharge. Most of these models use simple bucket-type expressions combined with several vertical water storage layers to describe near-surface water flow (Refsgaard and Storm, 1995; Wood et al., 1997; Koren et al., 2004; Samaniego et al., 2010; Niu et al., 2011). Due to the limitation in computational capability, all traditional hydrologic models simplify water flow processes by ignoring lateral groundwater flow. Thus, such models inevitably fall short of characterizing subsurface groundwater dynamics (Beven et al., 1984; Liang et al., 1994; Clark et al., 2015).

The implicit groundwater representations in traditional hydrologic models show inadequacy in many aspects. ~~Water table~~ depth has a strong influence on near-surface water processes such as evapotranspiration (Chen and Hu, 2004; Yeh and Eltahir, 2005; Koirala et al., 2014). Moreover, water table fluctuations are known as a factor affecting runoff generation and thus ~~impacting~~ the prediction skill of catchment runoff (Liang et al., 2003; Chen and Hu, 2004; Koirala et al., 2014). Typical hydrologic models also show inadequacy in simulating solute transport and retention at the catchment scale. For example, Van Meter et al. (2017) found that current nitrogen fluxes in rivers can be dominated by groundwater legacies. An over-simplified groundwater representation is inadequate for understanding travel time distributions (TTDs) at catchment scale and is therefore incapable of describing such legacy behavior (Benettin et al., 2015; Botter et al., 2010; Benettin et al., 2017). Moreover, stream-subsurface water interactions may be significant in modulating the human and environmental effects of nitrogen pollution (Azizian et al., 2017). Fianlly, to assess the response of groundwater to climate change, a more accurate groundwater representation including lateral subsurface flow is urgently needed (Scibek and Allen, 2006; Green et al., 2011; Ferguson et al., 2016).

Parallel to that, numerous groundwater models have been developed, which allow for both steady-state and transient ground-water flow in three dimensions with complex boundaries and a complex representation of sources and sinks. A variety of numerical codes are available such as MODFLOW (Harbaugh et al., 2000), FEFLOW (Diersch, 2013) and OpenGeoSys (Kolditz et al., 2012). Groundwater models usually ~~contain a mechanistic or physically-based~~ represent~~ation of~~ subsurface ~~physics,~~ but fall short in providing good representation of surface and shallow soil processes. For example, models for predicting groundwater storage change under either climate change (e.g., global warming) or human-induced scenarios (e.g., agricultural pumping) ~~always~~ use a constant or linear expression to represent spatially distributed recharge (Danskin, 1999; Selle et al., 2013). The groundwater numerical models may contain some packages or interfaces to simulate surface water or unsaturated zone processes (Harbaugh et al., 2000; Kalbacher et al., 2012; Delfs et al., 2012). Moreover, parameterization of topographical and geological parameters is a big challenge due to the strong spatial and temporal heterogeneity and lack of data (Moore and Doherty, 2006; Arnold et al., 2009).

In recent years, many integrated surface/subsurface hydrologic models (ISSHMs) have been developed. ISSHMs commonly focus on the comprehensive treatment of both the surface flow processes (e.g., 1D or 2D overland flow) and the subsurface flow processes (e.g., 1D or 3D Richards flow) using a two-way coupling procedure (Paniconi and Putti, 2015). Some of the highly recognized ISSHMs are InHM (Smerdon et al., 2007; VanderKwaak and Loague, 2001), Parflow (Maxwell and

Miller, 2005; Maxwell et al., 2015), OpenGeoSys (Kolditz et al., 2012; Delfs et al., 2012), tRIBS (Ivano et al., 2004), CATHY (Camporese et al., 2010), GSFLOW (Hunt et al., 2013; Markstrom et al., 2008), HydroGeoSphere (Hwang et al., 2014; Therrien et al., 2010), MIKE SHE (Graham and Butts, 2005), MODHMS (Panday and Huyakorn, 2004; Phi et al., 2013), GEOtop (Rigon et al., 2006), IRENE (Spanoudaki et al., 2009), CAST3M (Weill et al., 2009), PIHM (Kumar et al., 2009; Qu and Duffy, 2007), PAWS (Shen and Phanikumar, 2010). Although the methods for subsurface flow in ISSHMs are commonly based on saturated/unsaturated groundwater flow equations, the approaches for surface flow are inevitably based on some approximations and conceptualizations (e.g., kinematic wave approximation, 1D rill flow, etc). Besides, the modeling skill of reproducing distributed groundwater head dynamics at regional scale is always neglected and seldom assessed by the data (e.g., groundwater head, tracer, etc). The applications of these ISSHMs in the literature are mainly focusing on the field and small watershed scale, while the assessment of modeled groundwater heads dynamics at larger scales can only be found in very few publications (Goderniaux et al., 2009; Sutanudjaja et al., 2011). At this larger scale, i.e., regional scale, most of the ISSHMs are based on a continuity of pressure and flux on the surface water/groundwater (SW/GW) interface, while the momentum balance condition is always missing (Paniconi and Putti, 2015). Some of ISSHMs apply a storage-excess runoff generation concept, whereby the runoffs are normalized as storage-excess runoff through solving Richards equation combined with a boundary condition switching method. Then, the generated runoffs are routed into streams by a routing algorithm. These models can simulate the dynamic interaction of different processes within SW/GW components, e.g., the interaction of soil moisture and groundwater head (Cuthbert et al., 2013; Maxwell et al., 2015; Rihani et al., 2010; Sutanudjaja et al., 2014) as well as the storage-runoff correlation (VanderKwaak and Loague, 2001; Liang et al., 2003; Huntington and Niswonger, 2012; Koirala et al., 2014; Fang and Shen, 2017), etc.

Typical hydrologic models, like mHM (Samaniego et al., 2010; Kumar et al., 2013b), VIC (Liang et al., 1994) and HBV (Lindström et al., 1997), are good at predicting quantities like discharge but, as mentioned above, are highly conceptualized and ~~there suffering from~~ interpretability ~~of~~ certain processes (e.g., groundwater storage and heads). ~~M~~ore mechanistic ISSHMs, like Parflow, CATHY, and HydroGeoSphere, are highly interpretable but show consistently worse performance than typical hydrologic models when predicting runoff (Gulden et al., 2007; Paniconi and Putti, 2015). These different abilities of typical hydrologic models vs. the more mechanistic ISSHMs are caused by the different challenges that are posed by the different compartments of the terrestrial water cycle. One of the main challenges in the surface and near-surface storage is process uncertainty, with processes like evapotranspiration, land use, land cover, snow pack, are extremely complex and dynamic. The process uncertainty decreases as one goes deeper into the subsurface storage. In the subsurface storage, hydrological processes are relatively well understood and therefore conceptually simpler. Meanwhile, the data uncertainty becomes more significant in the deep subsurface storage compared to the shallow storage. Moreover, a recent study reveals the strong spatial and temporal heterogeneity of processes and properties ~~on~~ SW/GW interface, and underlines the importance of quantifying variability across several scales ~~on~~ SW/GW interface and its significance to water resources management (McLachlan et al., 2017).

In this study, we therefore coupled the Mesoscale Hydrologic Model (mHM v5.7) (Samaniego et al., 2010; Kumar et al., 2013b) with ~~a thermo-hydro-mechanical-chemical (THMC)~~ simulator OpenGeoSys (OGS) (Kolditz et al., 2012, 2016) with ~~an~~ overall aim of modelling regional-scale groundwater flow dynamics. mHM has ~~been~~ demonstrated its preeminence in

coping with process uncertainty in near-surface zone while providing excellent discharge prediction (Huang et al., 2017). On the other hand, OGS has demonstrated its ability of dealing with data uncertainty in aquifers. With these two well-tested codes, we want to answer the following scientific questions: can spatially distributed groundwater heads and their dynamics be reasonably captured by expanding the abilities of a surface hydrologic model like mHM at the regional scale, all while conserving its excellence in predicting discharge? can spatially resolved groundwater recharge estimates provided by mHM, improve the prediction of head measurements of groundwater models like OGS? To answer these questions, we applied the coupled model mHM#OGS v1.0 in a central German meso-scale catchment (850 km^2), and evaluated the model skills using measurements of streamflow and groundwater heads from several wells located in the study area. The coupled (surface) hydrologic and groundwater model (mHM#OGS v1.0) is our first attempt toward the development of a large-scale coupled modeling system with the aim to analyze the spatio-temporal variability of groundwater flow dynamics at a regional scale.

The paper is structured as follows. In the next section, we describe the model concept, model structure as well as coupling schematic. In Section 3, the study area and model setup used in this study are comprehensively illustrated. In Section 4, we present the simulation results of mHM#OGS v1.0 in. In the Section 5, we discuss model results as well as advantages and limitations of current modeling approach.

2 Model description

2.1 mesoscale Hydrologic Model (mHM v5.7)

The mesoscale Hydrologic Model (mHM, www.ufz.de/mhm) is a spatially explicit distributed hydrologic model that uses grid cells as a primary modeling unit, and accounts for the following processes: canopy interception, snow accumulation and melt-ing, soil moisture dynamics, infiltration and surface runoff, evapotranspiration, subsurface storage and discharge generation, deep percolation, baseflow, discharge attenuation as well as flood routing (Figure 1). The runoff generation applies a robust scheme which routes runoff in upstream cells along river network using the Muskingum-Cunge algorithm. The model is driven by daily meteorological forcings (e.g., precipitation, temperature) utilizes observable physical properties or signals (e.g., soil textural, vegetation, and geological properties) to infer the spatial variability of the required parameters. mHM is an open-source project written in Fortran 2008. Parallel versions of mHM OpenMP.

A unique feature of mHM is the application of Multiscale Parameter Regionalization (MPR). The MPR method accounts for subgrid variabilities physical characteristics such as topography, soil and vegetation. The model for hydrological simulations at various spatial scales (Samaniego et al., 2010; Kumar et al., 2013a, b; Rakovec et al., 2016a, b; Samaniego et al., 2017). mHM three levels to better represent the spatial variability of state and inputs variables. The effective parameters different spatial scales are dynamically linked by a physically-based upscaling scheme. Detailed description of MPR as well as formulations governing hydrological processes Samaniego et al. (2010) and Kumar et al. (2013b).
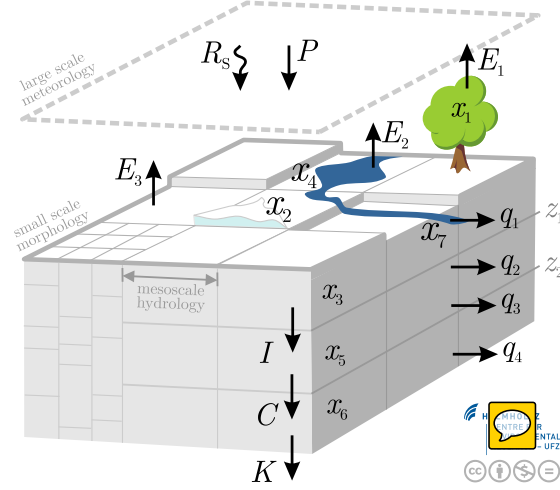
Figure 1. The concept of the mesoscale hydrologic model mHM.

Below, we listed the ~~formulas~~ that describe near-surface processes in the deep soil ~~layer~~ and groundwater layer. The comprehensive equation ~~system~~ of mHM can be found in Samaniego et al. (2010). Here, we only listed the equations relevant ~~to this study.~~ In the subsurface reservoir, which is the second ~~layer of the~~ vertical layers (x_5 in Figure 1), interflow is partitioned into fast interflow (q_2) and slow interflow (q_3):

$$q_2(t) = max\{I^2(t) + x_5(t-1) - \beta_1(z_2 - z_1),\, 0\}\beta_2 \tag{1}$$

$$q_3(t) = \beta_3(x_5(t-1))^{\beta_4} \tag{2}$$

where $q_2(t)$ is fast interflow at time t ~~(mm d⁻¹)~~, I is the infiltration capacity [mm d^{-1}], x_5 is depth of water storage in the deep soil reservoir [mm], β_1 is maximum holding capacity of the deep soil reservoir, z_i is depth of subsurface layer i, β_2 is fast recession constant, $q_3(t)$ is slow interflow at time t ~~[mm d⁻¹]~~, β_3 is slow concession constant, β_4 is exponent that quantifies the degree of non-linearity of the cell response.

The groundwater recharge is equivalent to the percolation to the groundwater reservoir (the third ~~of the~~ vertical layer~~s~~, see x_6 in Figure 1). The groundwater recharge $C(t)$ can be expressed by

$$C(t) = \beta_5 x_5(t-1) \tag{3}$$

where $C(t)$ is groundwater recharge ~~at~~ cell i [mm d^{-1}], β_5 is effective percolation rate.

In the groundwater reservoir, baseflow is generated following a linear relationship between storage and runoff:

$$q_4(t) = \beta_6 x_6(t-1) \tag{4}$$

where $q_4(t)$ is baseflow [mm d^{-1}], β_6 is baseflow recession rate, x_6 is depth of groundwater reservoir [mm].

The runoff from upstream grid and internal runoff ~~at~~ cell i are routed into streams using the Muskingum algorithm:

$$Q_i^1(t) = Q_i^1(t-1) + c_1(Q_i^0(t-1) - Q_i^1(t-1)) + c_2(Q_i^0(t) - Q_i^0(t-1)) \tag{5}$$

5

with

$$Q_i^0(t) = Q_{i'}(t) + Q_{i'}^1(t) \tag{6}$$

$$c_1 = \frac{\Delta t}{\kappa(1-\xi) + \frac{\Delta t}{2}} \tag{7}$$

$$c_2 = \frac{\frac{\Delta t}{2} - \kappa\xi}{\kappa(1-\xi) + \frac{\Delta t}{2}} \tag{8}$$

5   where Q_i^0 and Q_i^1 denote the runoff entering and leaving the river reach located ~~on~~ cell i respectively [mm d^{-1}], $Q_{i'}$ is the contribution from the upstream cell i' [mm d^{-1}], κ is Muskingum travel time parameter, ξ is the Muskingum attenuation parameter, Δt is time ~~interval in hours~~ [hr], t is time index for each Δt interval.

2.2 OpenGeoSys (OGS)

OpenGeoSys (OGS) is an open-source project with the aim of developing robust numerical methods for the simulation of
10   Thermo-Hydro-Mechanical-Chemical (THMC) processes in porous and fractured media. OGS is written in C++ with a focus on the finite element analysis of coupled multi-field problems. Parallel versions of OGS are available ~~based on both MPI and OpenMP concepts~~ (Wang et al., 2009; Kolditz et al., 2012; Wang et al., 2017). To date, two OGS versions are available ~~for use. These are~~ OGS5 (https://github.com/ufz/ogs5) and OGS6 (https://github.com/ufz/ogs). In this study, the term "OpenGeoSys (OGS)" represents OGS5 if ~~there is no special instruction~~.

15   OGS has been successfully applied in different fields such as water resources management, hydrology, geothermal energy, energy storage, CO_2 storage, and waste deposi~~tion~~ (Kolditz et al., 2012; Shao et al., 2013; Gräbe et al., 2013; Wang et al., 2017). In the field of hydrology / hydrogeology, OGS has been applied to ~~various topics such as~~ regional groundwater flow and transport (Sun et al., 2011; Selle et al., 2013), contaminant hydrology (Beyer et al., 2006; Walther et al., 2014), reactive transport (Shao et al., 2009; He et al., 2015), ~~and~~ sea water intrusion (Walther et al., 2012), etc.

20   ~~Here we list the governing equations of~~ saturated groundwater flow~~, which are relevant in this study. They can be expressed as~~:

$$S\frac{\partial \psi_p}{\partial t} = -\nabla \cdot \boldsymbol{q} + q_s \tag{9}$$

$$\boldsymbol{q} = -K_s\nabla(\psi_p - z) \tag{10}$$

where S is specific storage ~~for~~ confined aquifer and specific yield ~~for~~ unconfined aquifer [1/L], ψ_p is the pressure head in porous
25   media [L], t is time[T], $\boldsymbol{q}$ is the ~~Darcy flux~~ (LT^{-1}), q_s is a source/sink term (T^{-1}), K_s is the saturated hydraulic conductivity tensor [LT^{-1}], z is the vertical coordinate [L].

2.3 Coupling mechanism

The coupled model mHM#OGS v1.0 is developed to simulate SW/GW flow in one or more catchments by simultaneously calculating flow across the land surface and within ~~subsurface materials~~. mHM#OGS v1.0 simulates flow within three hydro-
30   logical regions. The first region is limited by the upper bound of plant canopy and the ~~lower bound~~ of the soil zone ~~bottom~~.

6

a) Original structure of mHM
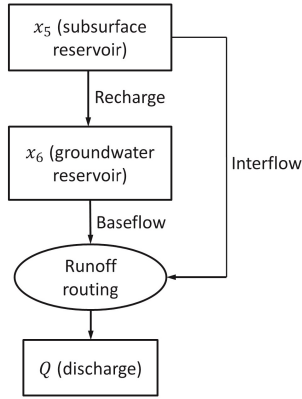
b) Structure of coupled model (mHM#OGS)
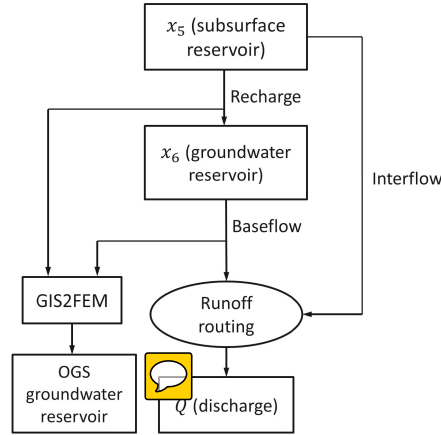
c) Schematic of coupling interface GIS2FEM
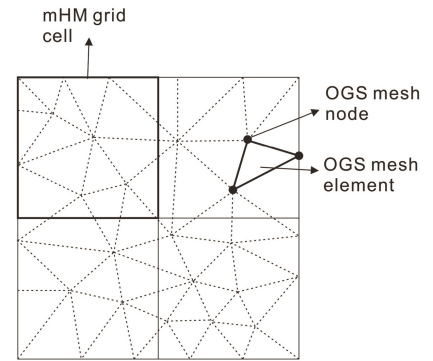
Figure 2. ~~The~~ schematic of the coupled model mHM#OGS v1.0. a) ~~the~~ original structure of vertical layered reservoir of mHM; b) ~~the~~ structure of coupled model (mHM#OGS v1.0). c) Illustration of data interpolation and transformation through the coupling interface GIS2FEM. For sake of simplicity, the figure only displays mHM layers relevant to this study, and neglect the other mHM layers (~~e.g.,~~ x_1 - x_4). Grid-based mHM fluxes (e.g., GW recharge and baseflow) are linear interpolated to top surface of OGS mesh, and further transferred into volumetric values ~~by face integration calculation, which are~~ directly assigned to OGS surface mesh nodes.

The second region includes open-channel water, such as streams. The third region is the saturated ~~groundwater~~ aquifer. mHM is used to simulate the processes in the first and second regions, while OGS is used to simulate the hydrological processes in the third region.

The basic idea is to feed fluxes generated by mHM (e.g., distributed groundwater recharge ~~and baseflow~~) to the OGS mesh surface as ~~outer forcings~~ through a coupling interface GIS2FEM (Figure 2). The two models are ~~performed~~ separately and sequentially with usually different temporal (e.g., daily in mHM and weekly or monthly in OGS) and spatial resolutions (e.g., ~~larger grid cell size~~ in mHM and smaller ~~element size~~ in OGS). The original vertical layered reservoirs in mHM, ~~e.g.,~~ the soil-zone ~~reservoir~~, subsurface ~~reservoir~~ and groundwater reservoir are preserved, implying that all well tested features of mHM (e.g., MPR, infiltration-runoff partitioning) are fully preserved in the coupled model.

To illustrate the coupling mechanism in detail, we itemized the coupling workflow in below.

1. mHM is run independent of OGS to calculate land surface fluxes.

   Using a gridded ~~observations of~~ meteorological forcings (precipitation, temperature, and potential evapotranspiration), the grid-based distributed infiltration rates (e.g., groundwater recharge) and runoff components (e.g., interflow, baseflow) are thereby estimated and saved as mHM output files. The original linear groundwater reservoir (depth x_6 in Figure 1) is used to estimate baseflow. Moreover, MPR is used in the calibration process such that subgrid variabilities can be validly

calculated. ~~The details of physical basis and parameterization scheme in mHM can be found in Section 2.1.~~ The spatially distributed groundwater recharge and total routed baseflow are written into raster files for later use.

2. After mHM run ~~was~~ finished, the step-wise routed baseflow estimated by mHM ~~are~~ transformed to distributed ~~baseflow along OGS~~ stream ~~network~~.

~~The stream conceptions within~~ mHM and OGS ~~are~~ slightly different~~, in terms that the~~ stream in mHM ~~is~~ based on pre-processing of DEM data and a routing scheme, while ~~in~~ OGS ~~by~~ an explicit predefined river geometry. In OGS, each reach of the stream network is defined by a polyline in an OGS geometry file. To coordinate the two different concept~~ions~~, we transfer the total routed baseflow (estimated by mHM) to distributed baseflow along OGS streams by distributing it uniformly along the predefined stream network in OGS. The detailed description of stream network in OGS can be found in Section 3.3. This approach is ~~based on the fact that due to~~ lack of data ~~(e.g., river bed conductance, tracer tracking, etc)~~, the spatial pattern of baseflow along streams is uncertain. Based on ~~the~~ mass conservation criteria, we made the assumption that baseflow is uniformly distributed along streams such that the step-wise water balance is guaranteed.

3. The distributed groundwater recharge generated ~~from~~ mHM are fed to the coupling interface GIS2FEM, and further transferred to the upper surface boundary conditions of the OGS model.

The coupling interface GIS2FEM is used to interpolate and transfer mHM grid-based fluxes to OGS nodal flux values. After reading a raster file of mHM generated fluxes, the interface GIS2FEM interpolates the flux value to the top surface elements of the OGS mesh. For each surface element, if its centroid is within the range of mHM grid cell, the flux of this grid cell is assigned to the corresponding surface element in OGS mesh. After all top surface elements ~~being~~ processed, GIS2FEM will ~~take the face integration calculation, by which~~ the recharge data and baseflow ~~are converted~~ into nodal source terms and assigned to the corresponding OGS mesh nodes (Figure 2c).

4. After mHM-generated recharge and baseflow ~~were~~ successfully transferred to boundary conditions ~~on~~ upper-surface of OGS mesh, the groundwater model ~~will~~ run ~~subsequently~~ to simulate groundwater flow and transport ~~processes~~.

3 Study area and model setup

We use a meso-scale catchment (about 850 km^2) upstream of the Nägelstedt gauge located in central Germany to ~~establish and assess our~~ model (Figure 3). The Nägelstedt catchment comprises the headwaters of the Unstrut river ~~basin. The Unstrut river basin is a sedimentary basin of Unstrut river~~, a ~~left~~ tributary of ~~the~~ Saale. It is selected ~~in~~ this study because there ~~are~~ many groundwater monitoring wells operated by Thuringian State office for the Environment and Geology (TLUG) and the Collaborative Research Center AquaDiva (Küsel et al., 2016). ~~Morphologically, the terrain~~ elevation within the catchment ~~is in a~~ range ~~of~~ 164 m and 516 m, whereby the higher regions are in the west and south ~~as part of~~ the forested hill chain of the Hainich (Figure 3). The Nägelstedt catchment is one of the most intensively used agricultural regions in Germany. In terms
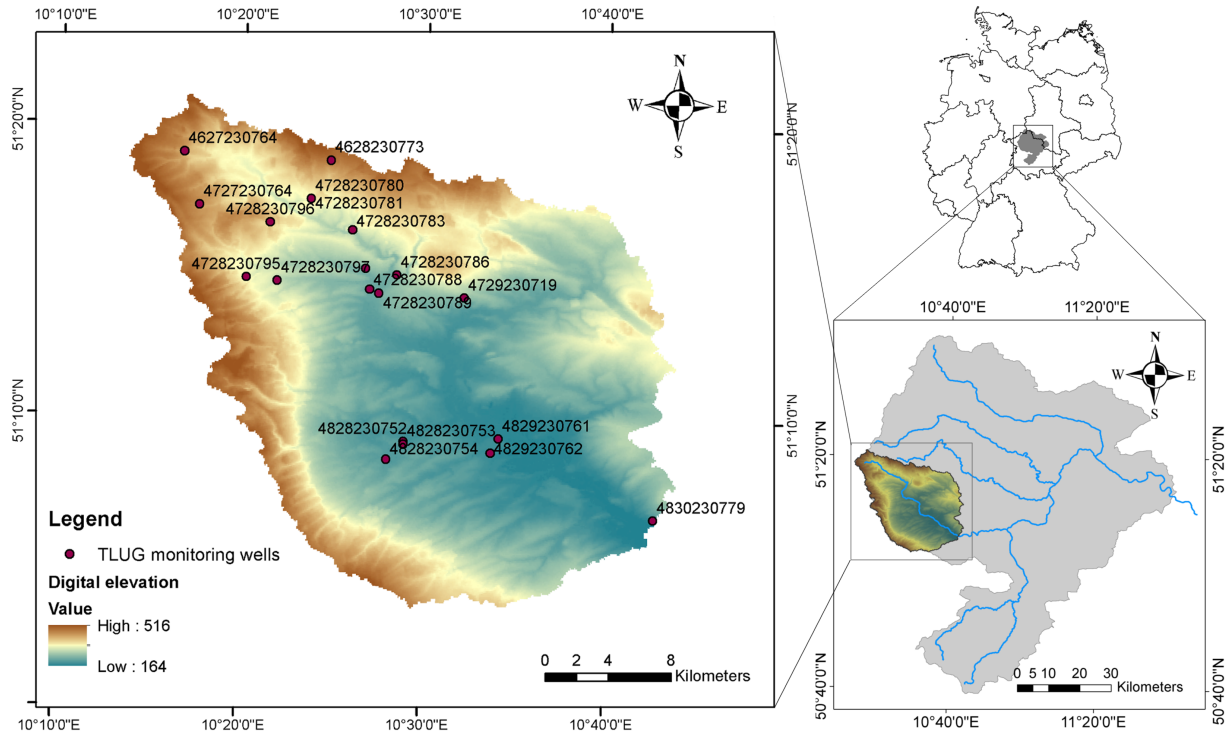
Figure 3. The Nägelstedt catchment used as the test catchment for ~~this~~ model. The left map shows ~~elevation~~ and locations of monitoring wells used in this study. The lower right map shows the relative location of Nägelstedt catchment ~~in~~ Unstrut basin. The upper right map shows the location of Unstrut basin in Germany.

of water supply, about 70% of the water requirement is satisfied by groundwater (Wechsung, 2005). About 17% of the land in this region is forested area, 78% is covered by crop and grassland and 4% is ~~housing~~ and transport area. The mean annual precipitation in this area is about 660 mm.

In this study, mHM runs are executed for a time period of 35 years (from January 1, 1970 to December 30, 2004), with the
5   period 1970 - 1974 being used ~~as a~~ spin-up ~~period~~. OGS is run for the period from January 1, 1975 to December 30, 2005. mHM is run with a daily time step, while OGS is run with a monthly time step. The resolution of mHM grid cells is 500 m × 500 m. The spatial resolution of OGS mesh is set to 250 m × 250 m in horizontal direction and 10 m in vertical direction over the whole domain. The fluxes are interpolated from coarser mHM grid to finer OGS surface element ~~through~~ GIS2FEM (Figure 2c). The detailed input data and parameter set to run both models are detailed in the following sections.

10 **3.1   Meteorological forcings and morphological properties**

We started the modeling by performing the daily simulation of mHM to calculate near-surface hydrological processes. The mHM model is forced by daily meteorological forcings, including distributed precipitation and atmosphere temperature. The
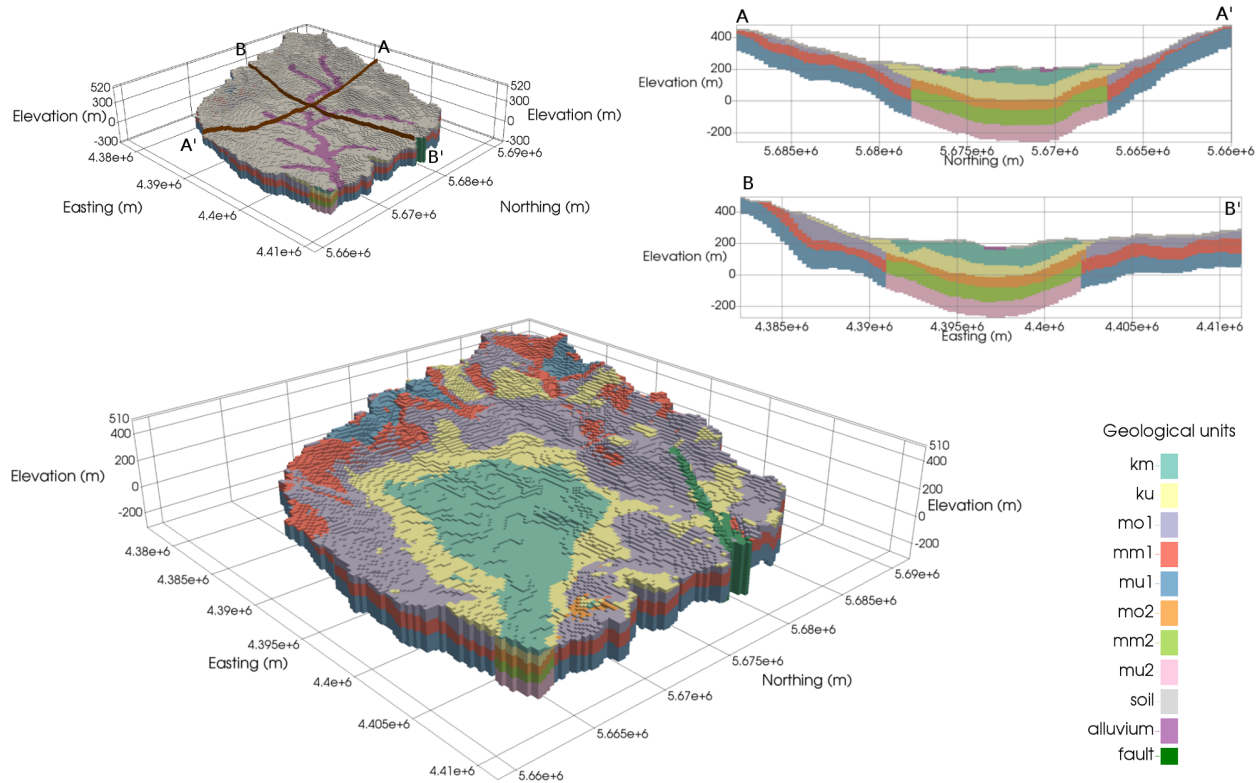
9

Figure 4. Three-dimensional and cross-section view of hydrogeologic zonation in the Nägelstedt catchment. The upper left figure ~~shows the complete geological characterization and zonation including~~ alluvium and soil zone. The upper right figure shows ~~the~~ geological ~~characterization along two~~ cross sections. The lower map shows the detailed zonation of geological sub-units beneath the soil zone and alluvium.

spatial patterns of precipitation and atmosphere temperature were based on point measurements of precipitation and atmosphere temperature at weather stations from the German Meteorological Service (DWD) . The point data at weather stations were subsequently krigged ~~into a 4 km~~ precipitation fields, and then downscaled to mHM grid cells. ~~Moreover, the~~ potential ET was ~~quantified based on~~ the method ~~from~~ Hargreaves and Samani (1985). Other datasets used in mHM are the digital elevation model (DEM) ~~data~~, which is the basis for deriving ~~properties like~~ slope, river beds, flow direction; soil and geological maps and meta-data such as sand and clay contents, bulk density, and dominant geological types; CORINE land-cover information (in the years 1990, 2000 and 2005); and discharge data at the outlet of catchment.

3.2 Aquifer properties

We used a stratified aquifer model to explicitly present heterogeneous distribution of hydraulic properties (~~e.g., K value~~, specific yield, specific storage). The stratified aquifer model is based on well log data and geophysical data from Thuringian State office
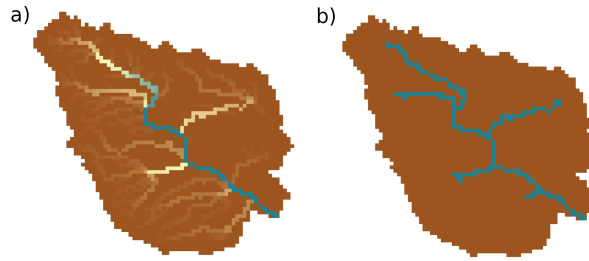
10

Figure 5. Illustration of stream network used in this study. a) Original stream network based on the streamflow routing algorithm of mHM; b) Processed stream network that are used in this study. The small tributaries where the runoff rates are below 1500 mm/month have been cut out from the original stream network.

for the Environment and Geology (TLUG). To convert the data format, we used the workflow developed by Fischer et al. (2015), by which the complex 3D geological model were converted into open-source VTK format file that can be read by OGS.

The dominant sediments in the study site are Muschelkalk (Middle Triassic) and Keuper (Middle and Late Triassic). Younger deposits from Tertiary and Quaternary are less important for the large scale hydrogeology of the basin. The Keuper deposits
5   mainly lie in the center of the Unstrut basin and act as permeable shallow aquifers. In the Nägelstedt catchment, the Keuper deposits are further classified into two geological sub-units: Middle Keuper (km) and low Keuper (ku) (see Figure 4). The Muschelkalk is marked by a prevailing marine environment and is subdivided into three sub-units Upper Muschelkalk (mo), Middle Muschelkalk (mm) and low Muschelkalk (mu). According to previous geological survey (Seidel, 2004), even the same sub-unit of Muschelkalk have a diverse hydraulic properties depending on their positions and depths. They are further divided
10 into sub-units with higher permeabilities, which are mo1, mm1 and mu1 (Figure 4), and sub-units with lower permeabilities, which are mo2, mm2 and mu2 (Figure 4). The uppermost layer with a depth of 10 m is set as a soil layer (Figure 4). A alluvium layer is set along the mainstream and major tributaries representing granite and stream deposits (Figure 4).

3.3   Boundary conditions

Based on the steep topography along the watershed divides, groundwater is assumed to be naturally separated and not able to
15 pass across the boundaries of the watershed. No-flow boundaries are imposed at the outer perimeters surrounding the basin as well as at the lower aquitard.

The stream network is delineated by processing a grid-based runoff raster file generated by mHM. The grid-based runoff is converted to a valid stream network compatible with OGS. The necessity of transferring mHM runoff raster file to OGS stream network has been elaborated in Section 2.3. Particularly in this case study, we cut out the small intermittent tributaries
20 by setting a threshold value of long-term averaged routed runoff. Only streams with a runoff rate higher than the threshold (in this case study, 1500 mm/month) are delineated as valid streams. In other words, we neglect the intermittent streams to the upper stream reaches (Figure 5). The preprocessed stream network consists of a main stream and four tributaries (Figure 5b). Each stream is defined as a polyline in OGS geometry file and comprises many consecutive nodes in OGS mesh. As mentioned

in Section 2.3, uniformly distributed baseflow rates were subsequently assigned to every OGS mesh nodes within the stream network.

3.4 Calibration procedure

The calibration of the coupled model mHM#OGS v1.0 follows a two-step procedure.

For the first step, mHM is calibrated independent of OGS for the period from 1970 to 2005 by matching observed runoff at the outlet of the catchment. The first 5 years are used as "spin-up" period to set up initial conditions in near-surface soil zone. The calibration workflow is a consecutive workflow where the parameters which affect the potential evapotranspiration, soil moisture, runoff and shallow subsurface flow were first calibrated until convergence criteria was matched. The calibration goodness is handled by means of calculating the Nash-Sutcliffe efficient (NSE):

$$NSE = 1 - \frac{\sum_{i=1}^{n} |(h_m - h_s)|_i^2}{\sum_{i=1}^{n} |(h_m - \bar{h}_m)|_i^2} \tag{11}$$

where h_s is the simulated groundwater head [m], $\bar{h}_m$ is the mean of measured groundwater head [m].

For the second step, the steady state groundwater model is calibrated to match the long-term mean of groundwater observations. The long term mean of recharge and baseflow estimated by mHM are fed to the steady-state groundwater model as boundary conditions. Meanwhile, the groundwater levels obtained from a couple of monitoring wells are averaged over the whole simulation period. The calibration of the steady-state groundwater model aims for the most plausible distribution of hydraulic conductivities. The intervals (i.e., upper and lower bounds) of adjustable parameters are taken from the literature (Wechsung, 2005; Seidel, 2004). Model-to-measurement matching is implemented by minimizing the objective function, which is the sum of weighted squared residuals of long-term mean of modeled groundwater heads and observed groundwater heads in this case. Goodness of fit between the simulated and observed long-term average groundwater levels is assessed by the root-mean-square error (RMSE).

3.5 Model evaluation and sensitivity analysis

Besides the observed discharge at the catchment outlet, we also used observed groundwater head time series in 19 monitoring wells distributed over the catchment to evaluate model performance. The K values are set to the optimized values from the steady-state model calibration. Meanwhile, the steady-state groundwater hydrographs are used as the initial condition for the transient groundwater model. For evaluating the predictive ability in terms of groundwater heads, the Pearson correlation coefficient R_{cor} and the inter-quantile range error QRE are used as two summary statistics. The (relative) inter-quantile range error QRE is defined by:

$$QRE = \frac{IQ_{7525}^{md} - IQ_{7525}^{dt}}{IQ_{7525}^{dt}} \tag{12}$$

where IQ_{7525}^{md} and IQ_{7525}^{dt} are the inter-quantile ranges of the time-series of modeling result and observations, respectively.

We also sought to quantify the effect of a spatially-distributed recharge on the simulated groundwater heads. For this purpose, we set up a reference scenario by spatially homogenizing mHM-generated recharge. To distinguish the two recharge scenarios,

we use the abbreviation "RR" to represent reference recharge scenario, and "mR" to represent mHM recharge scenario. The sensitivity analysis follows a two-step workflow. First, we calibrated the steady-state groundwater models in two recharge scenarios independently. Second, we conducted transient simulations by assigning the same values of storage parameters and compared their corresponding performances in two recharge scenarios. Despite the different spatial pattern of recharge and K values, all model parameters (e.g., specific yields, specific storage) and model inputs in the two scenarios are identical. The R_{cor} and QRE are used to assess model performances in the two respective simulations.

4 Results

4.1 Calibration

As the first step, mHM is calibrated independent of OGS. Monthly discharge data from January 1975 to December 2004 are used for model calibration. The calibration results indicate that mHM is capable to reasonably reproduce the time series of catchment discharge (Figure 6). The Nash–Sutcliffe model efficiency coefficient (NSE) is 0.88, while the Pearson correlation coefficient is 0.96 (Figure 6). Other fluxes like evaportransporation measured at eddy-covariance stations inside this area, also shows quite reasonable correspondence to the modeled estimation (Heße et al., 2017).

Subsequently, steady-state groundwater model is calibrated against long-term mean of groundwater heads using PEST (Doherty et al., 1994). Table 1 shows the calibrated hydraulic conductivities of each geological units. The upper and lower limit of each parameter are defined according to literature (Seidel, 2004; Wechsung, 2005). The calibrated conductivities in each geological zone are displayed in Table 1. The objective function of calibration, which is the sum of squared weighted residuals, converged from the initial value of 8625 m^2 to 464.74 m^2 after 114 total model runs.

Broadly speaking, the calibration results suggest that the groundwater model can plausibly reproduce the finite numbers of observed groundwater heads within the catchment. Figure 7 shows the 1-to-1 plot of simulated and observed groundwater heads (locations of those wells are shown in Figure 3). It can be observed that the model is capable of reproducing spatially-distributed groundwater heads in a wide range with an overall RMSE value of 6.33 m. The errors in simulated heads (Figure 7b) show that most of simulated head errors are within an interval of ±6 m. Nevertheless, there are some monitoring wells where the predictions are biased from observations due to the complex local geological formations around monitoring wells. No further attempt was made to add more model complexity to improve model-to-measurement match.

Simulated water table depth over the whole catchment using the calibrated K values is shown in Figure 7c. Broadly speaking, the calibrated model reasonably reproduced spatial groundwater table distribution. Groundwater table depth is as large as above 40 m in the higher southwestern and northern mountainous areas, whereas less than 5 m in the central lowlands from simulation results. The plausibility of steady-state simulation results can further be assessed through regionalized observations of groundwater heads (Wechsung, 2005).
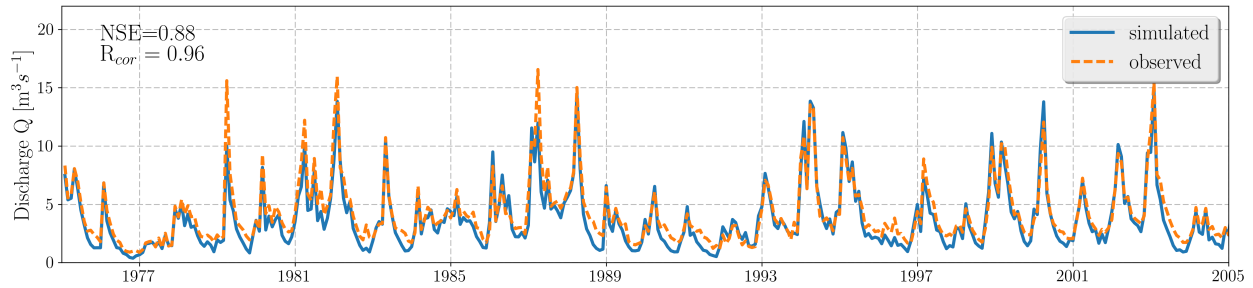
13

Figure 6. Observed and simulated monthly discharge at the outlet of Nagelstedt catchment.
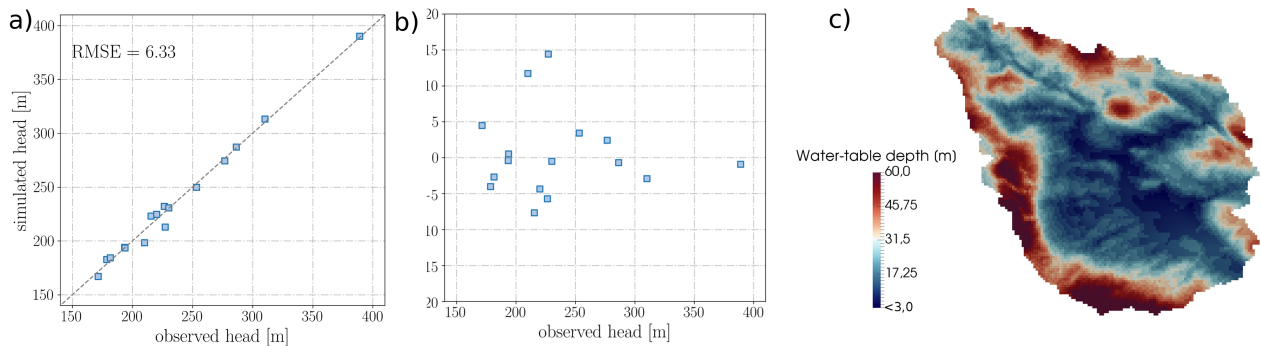

Figure 7. Illustration of steady-state groundwater model calibration and simulatied heads. (a) Observed and simulated groundwater head (including RMSE) ; (b) Difference between simulated and observed head related to the observaed head values; c) Simulated long term mean water table depth over Nägelstedt catchment.

4.2 Spatio-temporal patterns of recharge and baseflow

Groundwater recharge has an arbitrary behaviour depending on the sporadic, irregular, and complex features of storm rainfall occurrences, geological structure, and morphological features. The temporal and spatial variability of groundwater recharge and baseflow is estimated by mHM calculation with a period of 30 years from 1975 to 2005.

5   Figure 8 shows the spatial variability of groundwater recharge in three months: the early spring (March) (Figure 8a), late spring (May) (Figure 8b), and winter (January) (Figure 8c). The results indicate that the largest groundwater recharge may occur at mountainous areas. Largest recharge occurs in the upstream bedrock areas where dominant sedimentary is Muschelkalk with a relatively low hydraulic conductivity. The largest point-wise monthly groundwater recharge varies from 26 mm in early spring to 51 mm in late spring and 14 mm in winter. Besides, we evaluated the plausibility of groundwater recharge simulated

10   by mHM with other reference datasets. At the large scale, the simulated groundwater recharge from mHM agrees quite well with estimates from the Hydrological Atlas of Germany (Zink et al., 2017).
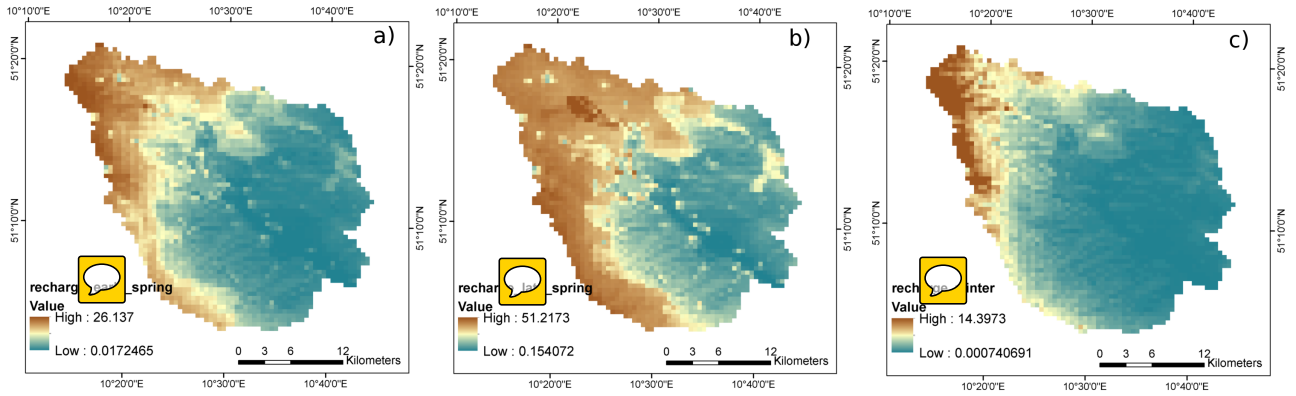
14

Figure 8. Spatial distributions of groundwater recharge in Nägelstedt catchment (unit: mm/month) (a) ~~during early spring~~, (b) ~~late spring~~, and (c) ~~winter of year~~ 2005.

<mark>The boxplot (Figure 9a) shows the degree of spread and skewness of the distributions of the monthly groundwater recharge and groundwater discharge. It reveals the long-term mean of groundwater inflow and outflow are balanced with the same monthly value of 8 mm/month. Due to the numerical error, a tiny difference of 2% between groundwater recharge and baseflow is observed in the boxplot. Nevertheless, we consider this bias to be within an acceptable interval.</mark> Figure 9b shows the distribution of monthly groundwater recharge and monthly baseflow. The figure indicates that the distribution of monthly groundwater recharge is skewed to the right, whereas the distribution of monthly baseflow is ~~unimodal~~. Figure 9c depicts the time series of groundwater recharge and baseflow, which further demonstrates that the deviation of monthly groundwater recharge is larger than the baseflow. This phenomenon further reveals the significant buffering effect of the linear groundwater storage in mHM.

4.3   Model evaluation against dynamic groundwater heads

In this subsection, the head observations ~~at~~ several monitoring wells ~~at~~ the catchment were used to evaluate the model performance. We analyze the discrepancies between the modeled groundwater heads ~~and their corresponding observed values in their anomalies~~ by ~~removing~~ long-term mean values $\overline{h}_{mod}$ and $\overline{h}_{obs}$. Four model skill scores including <mark>the mean value,</mark> <mark>the median value,</mark> the Pearson correlation coefficient R_{cor}, and the inter-quantile range error QRE are used to judge the model performance.

Five wells with different geological and morphological properties were ~~randomly~~ chosen ~~as samples~~ to test the effectiveness of our model. ~~Specifically, well~~ <mark>4728230786</mark> is located ~~at~~ northern upland and near the mainstream, whereas well <mark>4828230754</mark> is located ~~at~~ the southwestern lowland. As can be observed from Figure 10, they provide good fits between simulated ~~heads~~ and observed heads with the R_{cor} of 0.87 and 0.76, and the QRE of -23.34% and -1.65%, respectively. Well <mark>4628230773</mark> is located in lower Keuper ~~sediment~~, while well <mark>4728230781</mark> is located ~~at~~ upper Muschelkalk ~~sediment~~. ~~For the~~se two monitoring wells, simulation results are highly correlated with the observations with the R_{cor} of 0.71 and 0.81 in spite of their different geological properties (Figure 10). The simulation result at monitoring well <mark>4728230783</mark> located ~~at~~ northern mountainous area also has a
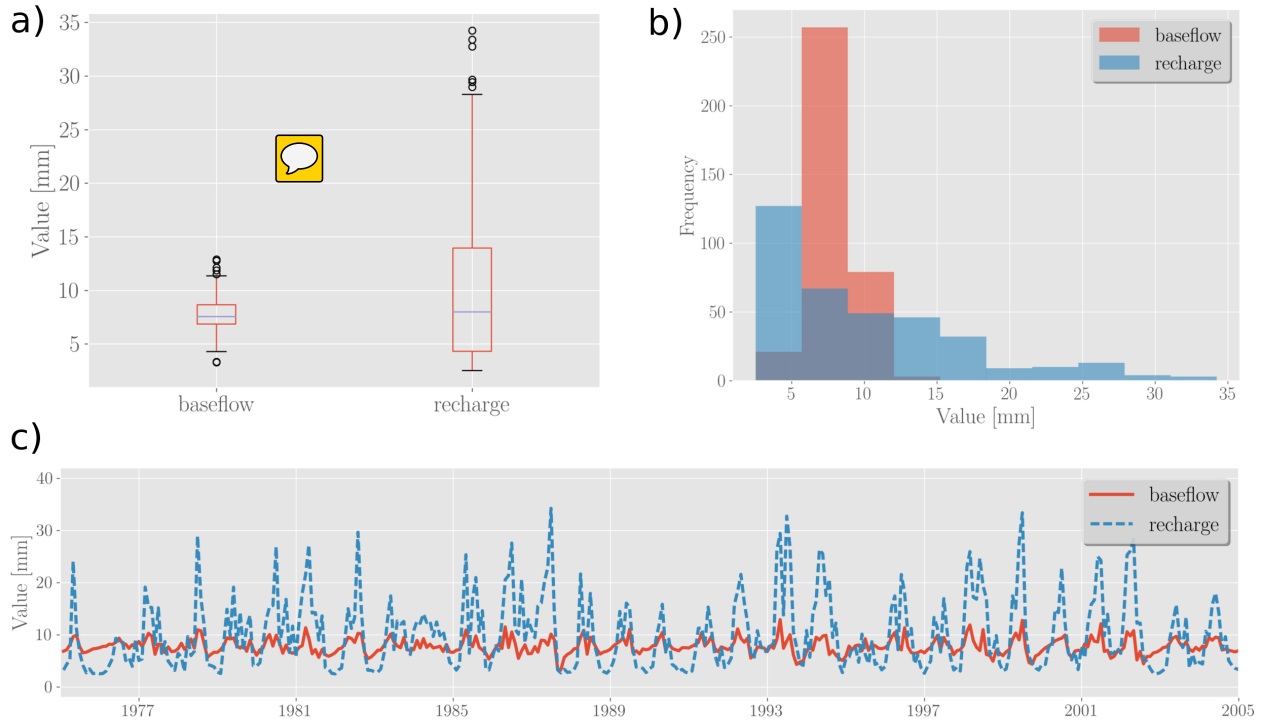
15

Figure 9. Analysis of groundwater inflow (recharge) and outflow (baseflow) over the Nägelstedt catchment. ~~a) Boxplot indicates spread, skewness, and outliers of groundwater recharge and baseflow.~~ b) ~~Histogram indicates the~~ distribution of groundwater balance components. c) Monthly time series of groundwater recharge and baseflow.

high correlation with the observation with a R_{cor} of 0.85 (Figure 10). In general, the model is capable of capturing the historical trend of groundwater dynamics, even though the mean values of simulation and observation may ~~mismatch~~ to some extent. Due to the limited spatial resolution and complex hydrogeological ~~locality~~ this degree of discrepancy is acceptable.

4.4 Model sensitivity to different recharge scenarios

5 As described in Section 3.5, we set up a reference recharge scenario (RR) in which the recharge is homogeneously distributed in space to assess the effect of spatial recharge pattern ~~towards~~ groundwater hydrographs. For the purpose of showing discrepancies ~~of model results~~ between two recharge scenarios, we compared the values of R_{cor} and |QRE| at each monitoring well between mR and RR (Figure 11). The mean value and the median value of R_{cor} and QRE are also calculated and shown in Figure 11. Figure 11a indicates that the correlation between observations and simulations using mR is higher than that using

10 RR, with the averaged vale 0.704 and 0.677, respectively. The standard deviations are nearly the same in both scenarios. Considering that the only difference between ~~mR and RR~~ is the spatial pattern ~~of recharge,~~ we ~~do~~ conclude that ~~the inclusion of~~

16

Table 1. Main hydraulic properties used for mHM#OGS v1.0.

Geological units	Hydraulic conductivity [m/s]			Specific yield [-]	Specific storage [m^{-1}]
	Lower limit	Upper limit	Calibrated value [m/s]		
km	1.0×10^{-6}	5.5×10^{-3}	1.493×10^{-5}	-	1×10^{-6}
ku	1.0×10^{-7}	3.4×10^{-3}	5.164×10^{-4}	-	1×10^{-6}
mo1	8.0×10^{-8}	2.0×10^{-3}	4.030×10^{-5}	0.10	1×10^{-6}
mm1	1.0×10^{-7}	9.0×10^{-4}	9.372×10^{-6}	-	1×10^{-6}
mu1	5.0×10^{-9}	2.0×10^{-4}	2.297×10^{-6}	-	1×10^{-6}
mo2	1.0×10^{-8}	5.0×10^{-4}	4.030×10^{-6}	-	1×10^{-6}
mm2	3.0×10^{-8}	9.0×10^{-5}	9.372×10^{-7}	-	1×10^{-6}
mu2	5.0×10^{-10}	2.0×10^{-5}	2.297×10^{-7}	-	1×10^{-6}
soil	5.0×10^{-5}	1.0×10^{-2}	3.068×10^{-4}	0.10	-
alluvium	4.0×10^{-4}	1.0×10^{-2}	1.026×10^{-3}	0.18	-

spatially-distributed recharge provides a solid improvement. The individual discrepancies of R_{cor} at well levels between the two scenarios are moderate.

Figure 11b shows the absolute values of inter-quantile range error (|QRE|) in simulations under two recharge scenarios (mR and RR), respectively. We found that the uncertainty of |QRE| is higher than R_{cor}, e.g., the |QRE| in two wells are abnormally higher than the other wells. The higher values of wells 4728230789 and 4627230764 may be caused by the proximity to model bounds, as the two wells locate near either river or outer bound. This phenomenon reveals the accurate quantification of fluctuation amplitude in certain locations are difficult due to the complex hydrogeological locality of individual wells. Nevertheless, 16 out of 19 wells have low inter-quantile range errors, with |QRE| values within an interval of ±40% in mR scenario. We also observe a smaller mean value of |QRE| in mR than in RR. The standard deviation of |QRE| in mR is also slightly smaller than RR. Those 19 monitoring wells cover geological zones of alluvium, Keuper, and Muschelkalk, and range from high mountains to lowlands all over the catchment. These results point towards the promising modeling capability of the model and highlight the moderately better simulation-to-observation match in mR.

Figure 12 displays the seasonality of groundwater heads over the whole catchment by means of calculating the long-term mean groundwater heads in spring, summer, autumn and winter, respectively. It indicates that in general, the possibility of groundwater flood event in spring and summer are higher than in autumn and winter. However, there can be observed a strong spatial variability over different morphological classes and within different geological groups. For example, the fluctuation amplitudes of groundwater heads in northern, eastern and southeastern mountainous areas are larger than the central plain areas. Considering the need for predicting groundwater flood and drought in extreme climate events, we select a meteorologically wet month (August 2002) and a meteorologically dry month (August 2003), and show the groundwater heads variation in these months. Figure 12e and Figure 12f show two scenes of groundwater head variations in wet season and dry season, respectively. In general, the groundwater heads in the wet season are higher than the long term mean values (Figure 12e). The

variation of groundwater heads in the dry season, however, shows a strong spatial variability. Such a strong spatial variability of groundwater heads variation has also been reported, e.g., by Kumar et al. (2016).

5 Discussion and conclusions

Our simulation results demonstrate that the coupled model mHM#OGS v1.0 can reproduce groundwater heads dynamics very

5 well in general. It is also able to reasonably reproduce fluctuation amplitudes of groundwater heads although with less accuracy. Compared to the good predictive capability of capturing the general trend behavior, the amplitude of head time series is hard to reproduce. This might be due to the fact that the local geological formations in the vicinity of monitoring wells (e.g, small apertures and rock cracks) may significantly alter local groundwater flow behavior, and thus further affect groundwater head fluctuations.

10   The results of this study demonstrate the successful application of the well-established mHM in estimating spatial heterogeneous groundwater recharge and baseflow at regional scale. In the spatial scale of 10^3 km^2 (the scale in this study), the distributed recharge estimated by mHM shows its priority over the reference homogeneous recharge. The mHM has been successfully applied at a larger scale over Europe (Thober et al., 2015; Kumar et al., 2013b; Zink et al., 2017; Rakovec et al., 2016b). The successful application of the coupled model in this study suggests a huge potential of extending the applicability

15 of mHM#OGS v1.0 to a larger scale (e.g., 10^4 - 10^6 km^2) or even global scale.

    The results of this study demonstrate a viable strategy for improving classic meso- to large-scale distributed hydrologic models, such as the current version of mHM (Samaniego et al., 2010; Kumar et al., 2013b), VIC (Liang et al., 1994), PCR-GLOBWB (Van Beek and Bierkens, 2009), WASMOD-M (Widén-Nilsson et al., 2007) . These distributed hydrologic models do not include the possibility of calculating spatio-temporal groundwater heads and are therefore not able to represent ground-

20 water head and storage dynamics in their groundwater compartment. The physical representation of groundwater flow is, however, relevant in future regional-scale and possibly global hydrologic models to accurately determine travel times, solute export from catchments and water quality in rivers (Botter et al., 2010; Benettin et al., 2015; Van Meter et al., 2017). The coupled model mHM#OGS v1.0 also provides a potential in predicting groundwater flood and drought in analyzing the dynamic behavior of groundwater heads. Thus, it could be a useful tool for understanding groundwater anomalies under extreme climate

25 conditions (Kumar et al., 2016; Marx et al., 2017).

    For example, building on previous work by Heße et al. (2017), who calculated Travel Time Distributions (TTDs) using mHM, we can now expand the range of their work to the complete hydrologic cycle beneath atmosphere, which is important for comprehensively understanding particle (e.g., pollutant) transport behavior and historical legacy in soil zone and groundwater storage (Beniston et al., 2014; Basu et al., 2010). mHM#OGS v1.0 fits well with the long-term simulation of nitrogen transport

30 in terrestrial water cycle based on the high reputation of two modeling codes in each other's fields. The coupled model is also able to evaluate surface water and groundwater storage change under different meteorological forcings, which allows the comprehensive evaluation of hydrologic response to climate change (e.g. global warming). Besides, the versatility of OGS also offers the possibility to address Thermo-Hydro-Mechanical-Chemical (THMC) coupling processes in large-scale hydrologic

cycles, which is significant for a wide range of real-world applications, including land subsidence, agricultural irrigation, nutrient circulation, salt water intrusion, drought, and heavy metal transport (Kalbacher et al., 2012; Selle et al., 2013; Walther et al., 2014, 2017).

In addition to improving the predictive abilities of mHM, we could also demonstrate some improvements for the groundwater model OGS. Our results showed a modest improvement using mHM generated recharge compared to a simpler, uniform recharge rate. We currently gain a strong advantage for the description of the top boundary condition, i.e. the recharge, which is temporal and spatially variable through the input of mHM. Even more, the recharge fluxes provided are based on mHM's phenomenological process description, which significantly better describes the surface level recharge fluxes than common approaches through empirical relations derived recharge rates. In the future, we will additionally advance in the description of water fluxes between surface and groundwater compartments through the coupled feedback between both simulation tools.

For this study, we focus our efforts on extending the mHM applicability in surface hydrology to subsurface hydrology in a simple one-way coupling . Consequently, we do not account for any feedback between river and groundwater head fluctuations. While being a simplification of reality, this approach has certain advantages. First, the one-way coupling can be regarded as a conservative approach, such that the parametrization process, which is one of the most salient features of mHM, remains fully intact. That way, we do not compromise any of its well-established features, such as calibration of model parameters at different scales and good runoff prediction ability, while getting in addition very good estimates of groundwater storage, flow paths and travel times. The lack of mHM to provide good estimates for these quantities has been noted in the past (see, e.g., Heße et al. (2017); Rakovec et al. (2016b)) and extends therefore the predictive abilities of mHM. Second, using such a one-way coupling will allow users of mHM to simply extend currently established catchment models and extend their abilities in the aforementioned way. Using a more sophisticated two-way coupling, would mean that user would have to re-establish these models almost from scratch. Third, even in the future, a one-way coupling would allow to easily expand the predictive power of a mHM catchment model if the practitioners later decide to do so, therefore leaving the option open. Finally, one-way coupling takes less computational consumption and achieves better numerical stability. In short, unlike a two-way coupling, the one-way coupling described here allows the user to expand the abilities of mHM without sacrificing any of its well-known and well-established properties. However, in a next step, we will try to incorporate a full, two-way coupling using the next version of mHM#OGS model. Via such a full coupling scheme, the dynamic interactions between overland flow and groundwater flow, as well as between soil moisture dynamics and groundwater dynamics can be explicitly modeled and investigated. This approach is open to a broader spectrum of calibration options, such as calibration using remotely sensed soil moisture data.

In conclusion, we can state that the coupled model mHM#OGS v1.0 fully preserves the predictive capability of discharge of mHM. In addition, it proves to be capable of reproducing groundwater head dynamics. The simulation results show a promising prediction ability via calibration and comparison to discharge and groundwater heads. Based on the historical match of discharge and groundwater heads in the case study, we would conclude that the coupled model mHM#OGS v1.0 is a valuable tool in coping with many challenging problems in the field of water management, including pollutant transport and legacy, climate change, and groundwater flood and drought.

References

Arnold, S., Attinger, S., Frank, K., and Hildebrandt, A.: Uncertainty in parameterisation and model structure affect simulation results in coupled ecohydrological models, Hydrology and Earth System Sciences, 13, 1789, 2009.

Azizian, M., Boano, F., Cook, P. L. M., Detwiler, R. L., Rippy, M. A., and Grant, S. B.: Ambient groundwater flow diminishes nitrate processing in the hyporheic zone of streams, Water Resources Research, 53, 3941–3967, doi:10.1002/2016WR020048, http://dx.doi.org/10.1002/2016WR020048, 2017.

Basu, N. B., Destouni, G., Jawitz, J. W., Thompson, S. E., Loukinova, N. V., Darracq, A., Zanardo, S., Yaeger, M., Sivapalan, M., Rinaldo, A., et al.: Nutrient loads exported from managed catchments reveal emergent biogeochemical stationarity, Geophysical Research Letters, 37, 2010.

Benettin, P., Kirchner, J. W., Rinaldo, A., and Botter, G.: Modeling chloride transport using travel time distributions at Plynlimon, Wales, Water Resources Research, pp. 3259–3276, doi:10.1002/2014WR016600, 2015.

Benettin, P., Soulsby, C., Birkel, C., Tetzlaff, D., Botter, G., and Rinaldo, A.: Using SAS functions and high-resolution isotope data to unravel travel time distributions in headwater catchments, Water Resources Research, 53, 1864–1878, doi:10.1002/2016WR020117, http://dx.doi.org/10.1002/2016WR020117, 2017.

Beniston, J. W., DuPont, S. T., Glover, J. D., Lal, R., and Dungait, J. A.: Soil organic carbon dynamics 75 years after land-use change in perennial grassland and annual wheat agricultural systems, Biogeochemistry, 120, 37–49, 2014.

Beven, K., Kirkby, M., Schofield, N., and Tagg, A.: Testing a physically-based flood forecasting model (TOPMODEL) for three UK catchments, Journal of Hydrology, 69, 119–143, 1984.

Beyer, C., Bauer, S., and Kolditz, O.: Uncertainty assessment of contaminant plume length estimates in heterogeneous aquifers, Journal of contaminant hydrology, 87, 73–95, 2006.

Botter, G., Bertuzzo, E., and Rinaldo, A.: Transport in the hydrologic response: Travel time distributions, soil moisture dynamics, and the old water paradox, Water Resources Research, 46, 1–18, doi:10.1029/2009WR008371, 2010.

Camporese, M., Paniconi, C., Putti, M., and Orlandini, S.: Surface-subsurface flow modeling with path-based runoff routing, boundary condition-based coupling, and assimilation of multisource observation data, Water Resources Research, 46, 2010.

Chen, X. and Hu, Q.: Groundwater influences on soil moisture and surface evaporation, Journal of Hydrology, 297, 285–300, 2004.

Clark, M. P., Fan, Y., Lawrence, D. M., Adam, J. C., Bolster, D., Gochis, D. J., Hooper, R. P., Kumar, M., Leung, L. R., Mackay, D. S., Maxwell, R. M., Shen, C., Swenson, S. C., and Zeng, X.: Improving the representation of hydrologic processes in Earth System Models, Water Resources Research, 51, 5929–5956, doi:10.1002/2015WR017096, http://dx.doi.org/10.1002/2015WR017096, 2015.

Cuthbert, M., Mackay, R., and Nimmo, J.: Linking soil moisture balance and source-responsive models to estimate diffuse and preferential components of groundwater recharge, Hydrology and Earth System Sciences, 17, 1003–1019, 2013.

Danskin, W. R.: Evaluation of the hydrologic system and selected water-management alternatives in the Owens Valley, California, vol. 2370, US Department of the Interior, US Geological Survey, 1999.

Delfs, J. O., Blumensaat, F., Wang, W., Krebs, P., and Kolditz, O.: Coupling hydrogeological with surface runoff model in a Poltva case study in Western Ukraine, Environmental Earth Sciences, 65, 1439–1457, doi:10.1007/s12665-011-1285-4, 2012.

Diersch, H.-J.: FEFLOW: finite element modeling of flow, mass and heat transport in porous and fractured media, Springer Science & Business Media, 2013.

Doherty, J. et al.: PEST: a unique computer program for model-independent parameter optimisation, Water Down Under 94: Groundwater/Surface Hydrology Common Interest Papers; Preprints of Papers, p. 551, 1994.

Fang, K. and Shen, C.: Full-flow-regime storage-streamflow correlation patterns provide insights into hydrologic functioning over the continental US, Water Resources Research, pp. 1–20, doi:10.1002/2016WR020283, http://doi.wiley.com/10.1002/2016WR020283, 2017.

5   Ferguson, I. M., Jefferson, J. L., Maxwell, R. M., and Kollet, S. J.: Effects of root water uptake formulation on simulated water and energy budgets at local and basin scales, Environmental Earth Sciences, 75, 1–15, 2016.

Fischer, T., Naumov, D., Sattler, S., Kolditz, O., and Walther, M.: GO2OGS 1.0: A versatile workflow to integrate complex geological information with fault data into numerical simulation models, Geoscientific Model Development, 8, 3681–3694, doi:10.5194/gmd-8-3681-2015, 2015.

10   Goderniaux, P., Brouyère, S., Fowler, H. J., Blenkinsop, S., Therrien, R., Orban, P., and Dassargues, A.: Large scale surface-subsurface hydrological model to assess climate change impacts on groundwater reserves, Journal of Hydrology, 373, 122–138, doi:10.1016/j.jhydrol.2009.04.017, http://dx.doi.org/10.1016/j.jhydrol.2009.04.017, 2009.

Gräbe, A., Rödiger, T., Rink, K., Fischer, T., Sun, F., Wang, W., Siebert, C., and Kolditz, O.: Numerical analysis of the groundwater regime in the western Dead Sea escarpment, Israel+ West Bank, Environmental earth sciences, 69, 571–585, 2013.

15   Graham, D. N. and Butts, M. B.: Flexible, integrated watershed modelling with MIKE SHE, Watershed models, 849336090, 245–272, 2005.

Green, T. R., Taniguchi, M., Kooi, H., Gurdak, J. J., Allen, D. M., Hiscock, K. M., Treidel, H., and Aureli, A.: Beneath the surface of global change: Impacts of climate change on groundwater, Journal of Hydrology, 405, 532–560, 2011.

Gulden, L. E., Rosero, E., Yang, Z. L., Rodell, M., Jackson, C. S., Niu, G. Y., Yeh, P. J. F., and Famiglietti, J.: Improving land-surface model hydrology: Is an explicit aquifer model better than a deeper soil profile?, Geophysical Research Letters, 34, 1–5,
20   doi:10.1029/2007GL029804, 2007.

Harbaugh, B. A. W., Banta, E. R., Hill, M. C., and Mcdonald, M. G.: MODFLOW-2000 , The U .S . Geological Survey modular graoundwater model — User guide to modularization concepts and the ground-water flow process, U.S. Geological Survey, p. 130, http://www.gama-geo.hu/kb/download/ofr00-92.pdf, 2000.

Hargreaves, G. H. and Samani, Z. A.: Reference crop evapotranspiration from temperature, Applied engineering in agriculture, 1, 96–99,
25   1985.

He, W., Beyer, C., Fleckenstein, J. H., Jang, E., Kolditz, O., Naumov, D., and Kalbacher, T.: A parallelization scheme to simulate reactive transport in the subsurface environment with OGS#IPhreeqc 5.5.7-3.1.2, Geoscientific Model Development, 8, 3333–3348, doi:10.5194/gmd-8-3333-2015, 2015.

Heße, F., Zink, M., Kumar, R., Samaniego, L., and Attinger, S.: Spatially distributed characterization of soil-moisture dynamics using travel-
30   time distributions, Hydrology and Earth System Sciences, 21, 549–570, doi:10.5194/hess-21-549-2017, http://www.hydrol-earth-syst-sci.net/21/549/2017/, 2017.

Huang, S., Kumar, R., Flörke, M., Yang, T., Hundecha, Y., Kraft, P., Gao, C., Gelfan, A., Liersch, S., Lobanova, A., Strauch, M., van Ogtrop, F., Reinhardt, J., Haberlandt, U., and Krysanova, V.: Evaluation of an ensemble of regional hydrological models in 12 large-scale river basins worldwide, Climatic Change, 141, 381–397, doi:10.1007/s10584-016-1841-8, https://doi.org/10.1007/s10584-016-1841-8, 2017.

35   Hunt, R. J., Walker, J. F., Selbig, W. R., Westenbroek, S. M., and Regan, R. S.: Simulation of Climate - Change effects on streamflow, Lake water budgets, and stream temperature using GSFLOW and SNTEMP, Trout Lake Watershed, Wisconsin, USGS Scientific Investigations Report., pp. 2013–5159, 2013.

Huntington, J. L. and Niswonger, R. G.: Role of surface-water and groundwater interactions on projected summertime streamflow in snow dominated regions: An integrated modeling approach, Water Resources Research, 48, 1–20, doi:10.1029/2012WR012319, 2012.

Hwang, H. T., Park, Y. J., Sudicky, E. A., and Forsyth, P. A.: A parallel computational framework to solve flow and transport in integrated surface-subsurface hydrologic systems, Environmental Modelling and Software, 61, 39–58, doi:10.1016/j.envsoft.2014.06.024, http://dx.doi.org/10.1016/j.envsoft.2014.06.024, 2014.

Ivano, V. Y., Vivoni, E. R., Bras, R. L., and Entekhabi, D.: Catchment hydrologic response with a fully distributed triangulated irregular network model, Water Resources Research, 40, n/a—-n/a, doi:10.1029/2004WR003218, http://dx.doi.org/10.1029/2004WR003218, 2004.

Kalbacher, T., Delfs, J. O., Shao, H., Wang, W., Walther, M., Samaniego, L., Schneider, C., Kumar, R., Musolff, A., Centler, F., Sun, F., Hildebrandt, A., Liedl, R., Borchardt, D., Krebs, P., and Kolditz, O.: The IWAS-ToolBox: Software coupling for an integrated water resources management, Environmental Earth Sciences, 65, 1367–1380, doi:10.1007/s12665-011-1270-y, 2012.

Koirala, S., Yeh, P. J.-F., Hirabayashi, Y., Kanae, S., and Oki, T.: Global-scale land surface hydrologic modeling with the representation of water table dynamics, Journal of Geophysical Research: Atmospheres, 119, 75–89, 2014.

Kolditz, O., Bauer, S., Bilke, L., Böttcher, N., Delfs, J. O., Fischer, T., Görke, U. J., Kalbacher, T., Kosakowski, G., McDermott, C. I., Park, C. H., Radu, F., Rink, K., Shao, H., Shao, H. B., Sun, F., Sun, Y. Y., Singh, A. K., Taron, J., Walther, M., Wang, W., Watanabe, N., Wu, Y., Xie, M., Xu, W., and Zehner, B.: OpenGeoSys: an open-source initiative for numerical simulation of thermo-hydro-mechanical/chemical (THM/C) processes in porous media, Environmental Earth Sciences, 67, 589–599, doi:10.1007/s12665-012-1546-x, http://link.springer.com/10.1007/s12665-012-1546-x, 2012.

Kolditz, O., Shao, H., Wang, W., and Bauer, S.: Thermo-hydro-mechanical-chemical processes in fractured porous media: modelling and benchmarking, Springer, 2016.

Koren, V., Reed, S., Smith, M., Zhang, Z., and Seo, D.-J.: Hydrology laboratory research modeling system (HL-RMS) of the US national weather service, Journal of Hydrology, 291, 297–318, 2004.

Kumar, M., Duffy, C. J., and Salvage, K. M.: A Second-Order Accurate, Finite Volume–Based, Integrated Hydrologic Modeling (FIHM) Framework for Simulation of Surface and Subsurface Flow, Vadose Zone Journal, 8, 873, doi:10.2136/vzj2009.0014, https://www.soils.org/publications/vzj/abstracts/8/4/873, 2009.

Kumar, R., Livneh, B., and Samaniego, L.: Toward computationally efficient large-scale hydrologic predictions with a multiscale regionalization scheme, Water Resources Research, 49, 5700–5714, doi:10.1002/wrcr.20431, 2013a.

Kumar, R., Samaniego, L., and Attinger, S.: Implications of distributed hydrologic model parameterization on water fluxes at multiple scales and locations, Water Resources Research, 49, 360–379, 2013b.

Kumar, R., Musuuza, J. L., Van Loon, A. F., Teuling, A. J., Barthel, R., Ten Broek, J., Mai, J., Samaniego, L., and Attinger, S.: Multiscale evaluation of the Standardized Precipitation Index as a groundwater drought indicator, Hydrology and Earth System Sciences, 20, 1117–1131, doi:10.5194/hess-20-1117-2016, 2016.

Küsel, K., Totsche, K. U., Trumbore, S. E., Lehmann, R., Steinhäuser, C., and Herrmann, M.: How deep can surface signals be traced in the critical zone? Merging biodiversity with biogeochemistry research in a central German Muschelkalk landscape, Frontiers in Earth Science, 4, 32, 2016.

Liang, X., Lettenmaier, D. P., Wood, E. F., and Burges, S. J.: A simple hydrologically based model of land surface water and energy fluxes for general circulation models, Journal of Geophysical Research: Atmospheres, 99, 14 415–14 428, 1994.

Liang, X., Xie, Z., and Huang, M.: A new parameterization for surface and groundwater interactions and its impact on water budgets with the variable infiltration capacity (VIC) land surface model, Journal of Geophysical Research, 108, 8613–8629, doi:10.1029/2002JD003090, http://www.agu.org/pubs/crossref/2003/2002JD003090.shtml, 2003.

Lindström, G., Johansson, B., Persson, M., Gardelin, M., and Bergström, S.: Development and test of the distributed HBV-96 hydrological
5   model, Journal of hydrology, 201, 272–288, 1997.

Markstrom, S. L., Niswonger, R. G., Regan, R. S., Prudic, D. E., and Barlow, P. M.: GSFLOW—Coupled Ground-Water and Surface-Water Flow Model Based on the Integration of the Precipitation-Runoff Modeling System (PRMS) and the Modular Ground-Water Flow Model (MODFLOW-2005), U.S. Geological Survey, p. 240, http://pubs.er.usgs.gov/publication/tm6D1, 2008.

Marx, A., Kumar, R., Thober, S., Zink, M., Wanders, N., Wood, E. F., Ming, P., Sheffield, J., and Samaniego, L.: Climate change alters
10   low flows in Europe under a 1.5, 2, and 3 degree global warming, Hydrology and Earth System Sciences Discussions, 2017, 1–24, doi:10.5194/hess-2017-485, https://www.hydrol-earth-syst-sci-discuss.net/hess-2017-485/, 2017.

Maxwell, R. M. and Miller, N. L.: Development of a coupled land surface and groundwater model, Journal of Hydrometeorology, 6, 233–247, doi:10.1175/JHM422.1, isi:000230393600001, 2005.

Maxwell, R. M., Condon, L. E., and Kollet, S. J.: A high-resolution simulation of groundwater and surface water over most of the continental
15   US with the integrated hydrologic model ParFlow v3, Geoscientific Model Development, 8, 923–937, http://www.geosci-model-dev.net/ 8/923/2015/, 2015.

McLachlan, P., Chambers, J., Uhlemann, S., and Binley, A.: Geophysical characterisation of the groundwater–surface water interface, Advances in Water Resources, 109, 302 – 319, doi:https://doi.org/10.1016/j.advwatres.2017.09.016, http://www.sciencedirect.com/science/ article/pii/S0309170817304463, 2017.

20   Moore, C. and Doherty, J.: The cost of uniqueness in groundwater model calibration, Advances in Water Resources, 29, 605–623, doi:10.1016/j.advwatres.2005.07.003, 2006.

Niu, G.-Y., Yang, Z.-L., Mitchell, K. E., Chen, F., Ek, M. B., Barlage, M., Kumar, A., Manning, K., Niyogi, D., Rosero, E., and Others: The community Noah land surface model with multiparameterization options (Noah-MP): 1. Model description and evaluation with local-scale measurements, Journal of Geophysical Research: Atmospheres, 116, 2011.

25   Panday, S. and Huyakorn, P. S.: A fully coupled physically-based spatially-distributed model for evaluating surface/subsurface flow, Advances in Water Resources, 27, 361–382, doi:https://doi.org/10.1016/j.advwatres.2004.02.016, http://www.sciencedirect.com/science/ article/pii/S030917080400017X, 2004.

Paniconi, C. and Putti, M.: Physically based modeling in catchment hydrology at 50: Survey and outlook, Water Resources Research, 51, 7090–7129, doi:10.1002/2015WR017780, http://dx.doi.org/10.1002/2015WR017780, 2015.

30   Phi, S., Clarke, W., and Li, L.: Laboratory and numerical investigations of hillslope soil saturation development and runoff generation over rainfall events, Journal of Hydrology, 493, 1–15, doi:https://doi.org/10.1016/j.jhydrol.2013.04.009, http://www.sciencedirect.com/science/ article/pii/S0022169413002813, 2013.

Qu, Y. and Duffy, C. J.: A semidiscrete finite volume formulation for multiprocess watershed simulation, Water Resources Research, 43, n/a—-n/a, doi:10.1029/2006WR005752, http://dx.doi.org/10.1029/2006WR005752, 2007.

35   Rakovec, O., Kumar, R., Attinger, S., and Samaniego, L.: Improving the realism of hydrologic model functioning through multivariate parameter estimation, Water Resources Research, 52, 7779–7792, 2016a.

Rakovec, O., Kumar, R., Mai, J., Cuntz, M., Thober, S., Zink, M., Attinger, S., Schäfer, D., Schrön, M., and Samaniego, L.: Multiscale and multivariate evaluation of water fluxes and states over European river basins, Journal of Hydrometeorology, 17, 287–307, 2016b.

Refsgaard, J. C. and Storm, B.: Mike SHE, Computer models of watershed hydrology, 1, 809–846, 1995.

Rigon, R., Bertoldi, G., and Over, T. M.: GEOtop: A Distributed Hydrological Model with Coupled Water and Energy Budgets, Journal of Hydrometeorology, 7, 371–388, doi:10.1175/JHM497.1, https://doi.org/10.1175/JHM497.1, 2006.

Rihani, J. F., Maxwell, R. M., and Chow, F. K.: Coupling groundwater and land surface processes: Idealized simulations to identify effects of terrain and subsurface heterogeneity on land surface energy fluxes, Water Resources Research, 46, 1–14, doi:10.1029/2010WR009111, 2010.

Samaniego, L., Kumar, R., and Attinger, S.: Multiscale parameter regionalization of a grid-based hydrologic model at the mesoscale, Water Resources Research, 46, 2010.

Samaniego, L., Kumar, R., Thober, S., Rakovec, O., Zink, M., Wanders, N., Eisner, S., Schmied, H. M., Sutanudjaja, E. H., Warrach-Sagi, K., et al.: Toward seamless hydrologic predictions across spatial scales, Hydrology and Earth System Sciences, 21, 4323, 2017.

Scibek, J. and Allen, D.: Modeled impacts of predicted climate change on recharge and groundwater levels, Water Resources Research, 42, 2006.

Seidel, G.: Geologie von Thüringen, Erdkunde, 58, 2004.

Selle, B., Rink, K., and Kolditz, O.: Recharge and discharge controls on groundwater travel times and flow paths to production wells for the Ammer catchment in southwestern Germany, Environmental Earth Sciences, 69, 443–452, doi:10.1007/s12665-013-2333-z, 2013.

Shao, H., Dmytrieva, S. V., Kolditz, O., Kulik, D. A., Pfingsten, W., and Kosakowski, G.: Modeling reactive transport in non-ideal aqueous–solid solution system, Applied Geochemistry, 24, 1287 – 1300, doi:https://doi.org/10.1016/j.apgeochem.2009.04.001, http://www.sciencedirect.com/science/article/pii/S0883292709000985, 2009.

Shao, H., Nagel, T., Roßkopf, C., Linder, M., Wörner, A., and Kolditz, O.: Non-equilibrium thermo-chemical heat storage in porous media: Part 2–A 1D computational model for a calcium hydroxide reaction system, Energy, 60, 271–282, 2013.

Shen, C. and Phanikumar, M. S.: A process-based, distributed hydrologic model based on a large-scale method for surface-subsurface coupling, Advances in Water Resources, 33, 1524–1541, doi:10.1016/j.advwatres.2010.09.002, http://dx.doi.org/10.1016/j.advwatres.2010.09.002, 2010.

Smerdon, B. D., Mendoza, C. A., and Devito, K. J.: Simulations of fully coupled lake-groundwater exchange in a subhumid climate with an integrated hydrologic model, Water Resources Research, 43, n/a–n/a, http://onlinelibrary.wiley.com/doi/10.1029/2006WR005137/full, 2007.

Spanoudaki, K., Stamou, A. I., and Nanou-Giannarou, A.: Development and verification of a 3-D integrated surface water–groundwater model, Journal of Hydrology, 375, 410–427, doi:https://doi.org/10.1016/j.jhydrol.2009.06.041, http://www.sciencedirect.com/science/article/pii/S0022169409003795, 2009.

Sun, F., Shao, H., Kalbacher, T., Wang, W., Yang, Z., Huang, Z., and Kolditz, O.: Groundwater drawdown at Nankou site of Beijing Plain: model development and calibration, Environmental Earth Sciences, 64, 1323–1333, doi:10.1007/s12665-011-0957-4, http://link.springer.com/10.1007/s12665-011-0957-4, 2011.

Sutanudjaja, E. H., Van Beek, L. P. H., De Jong, S. M., Van Geer, F. C., and Bierkens, M. F. P.: Large-scale groundwater modeling using global datasets: A test case for the Rhine-Meuse basin, Hydrology and Earth System Sciences, 15, 2913–2935, doi:10.5194/hess-15-2913-2011, 2011.

Sutanudjaja, E. H., Van Beek, L. P. H., De Jong, S. M., Van Geer, F. C., and Bierkens, M. F. P.: Calibrating a large-extent high-resolution coupled groundwater-land surface model using soil moisture and discharge data, Water Resources Research, 50, 687–705, doi:10.1002/2013WR013807, 2014.

Therrien, R., McLaren, R. G., Sudicky, E. A., and Panday, S. M.: HydroGeoSphere: A three-dimensional numerical model describing fully-integrated subsurface and surface flow and solute transport, Groundwater Simulations Group, University of Waterloo, Waterloo, ON, 2010.

Thober, S., Kumar, R., Sheffield, J., Mai, J., Schäfer, D., and Samaniego, L.: Seasonal Soil Moisture Drought Prediction over Europe Using the North American Multi-Model Ensemble (NMME), Journal of Hydrometeorology, 16, 2329–2344, doi:10.1175/JHM-D-15-0053.1, https://doi.org/10.1175/JHM-D-15-0053.1, 2015.

Van Beek, L. and Bierkens, M. F.: The global hydrological model PCR-GLOBWB: conceptualization, parameterization and verification, Utrecht University, Utrecht, The Netherlands, 2009.

Van Meter, K. J., Basu, N. B., and Van Cappellen, P.: Two centuries of nitrogen dynamics: Legacy sources and sinks in the Mississippi and Susquehanna River Basins, Global Biogeochemical Cycles, 31, 2–23, doi:10.1002/2016GB005498, 2017.

VanderKwaak, J. E. and Loague, K.: Hydrologic-response simulations for the R-5 catchment with a comprehensive physics-based model, Water Resources Research, 37, 999–1013, doi:10.1029/2000WR900272, 2001.

Walther, M., Delfs, J.-O., Grundmann, J., Kolditz, O., and Liedl, R.: Saltwater intrusion modeling: Verification and application to an agricultural coastal arid region in Oman, Journal of Computational and Applied Mathematics, 236, 4798 – 4809, doi:http://dx.doi.org/10.1016/j.cam.2012.02.008, http://www.sciencedirect.com/science/article/pii/S0377042712000659, fEMTEC 2011: 3rd International Conference on Computational Methods in Engineering and Science, May 9–13, 2011, 2012.

Walther, M., Solpuker, U., Böttcher, N., Kolditz, O., Liedl, R., and Schwartz, F. W.: Description and verification of a novel flow and transport model for silicate-gel emplacement, Journal of contaminant hydrology, 157, 1–10, 2014.

Walther, M., Graf, T., Kolditz, O., Liedl, R., and Post, V.: How significant is the slope of the sea-side boundary for modelling seawater intrusion in coastal aquifers?, Journal of Hydrology, 551, 648 – 659, doi:https://doi.org/10.1016/j.jhydrol.2017.02.031, http://www.sciencedirect.com/science/article/pii/S0022169417301105, investigation of Coastal Aquifers, 2017.

Wang, W., Kosakowski, G., and Kolditz, O.: A parallel finite element scheme for thermo-hydro-mechanical (THM) coupled problems in porous media, Computers & Geosciences, 35, 1631–1641, doi:10.1016/j.cageo.2008.07.007, http://linkinghub.elsevier.com/retrieve/pii/S0098300409000065, 2009.

Wang, W., Kolditz, O., and Nagel, T.: Parallel finite element modelling of multi-physical processes in thermochemical energy storage devices, Applied Energy, 185, 1954–1964, 2017.

Wechsung, F.: Auswirkungen des globalen Wandels auf Wasser, Umwelt und Gesellschaft im Elbegebiet, vol. 6, Weißensee Verlag, 2005.

Weill, S., Mouche, E., and Patin, J.: A generalized Richards equation for surface / subsurface flow modelling, Journal of Hydrology, 366, 9–20, doi:10.1016/j.jhydrol.2008.12.007, http://dx.doi.org/10.1016/j.jhydrol.2008.12.007, 2009.

Widén-Nilsson, E., Halldin, S., and Xu, C.-y.: Global water-balance modelling with WASMOD-M: Parameter estimation and regionalisation, Journal of Hydrology, 340, 105–118, 2007.

Wood, E. F., Lettenmaier, D., Liang, X., Nijssen, B., and Wetzel, S. W.: Hydrological modeling of continental-scale basins, Annual Review of Earth and Planetary Sciences, 25, 279–300, 1997.

Yeh, P. J. and Eltahir, E. A.: Representation of water table dynamics in a land surface scheme. Part I: Model development, Journal of climate, 18, 1861–1880, 2005.

Zink, M., Kumar, R., Cuntz, M., and Samaniego, L.: A high-resolution dataset of water fluxes and states for Germany accounting for parametric uncertainty., Hydrology & Earth System Sciences, 21, 2017.
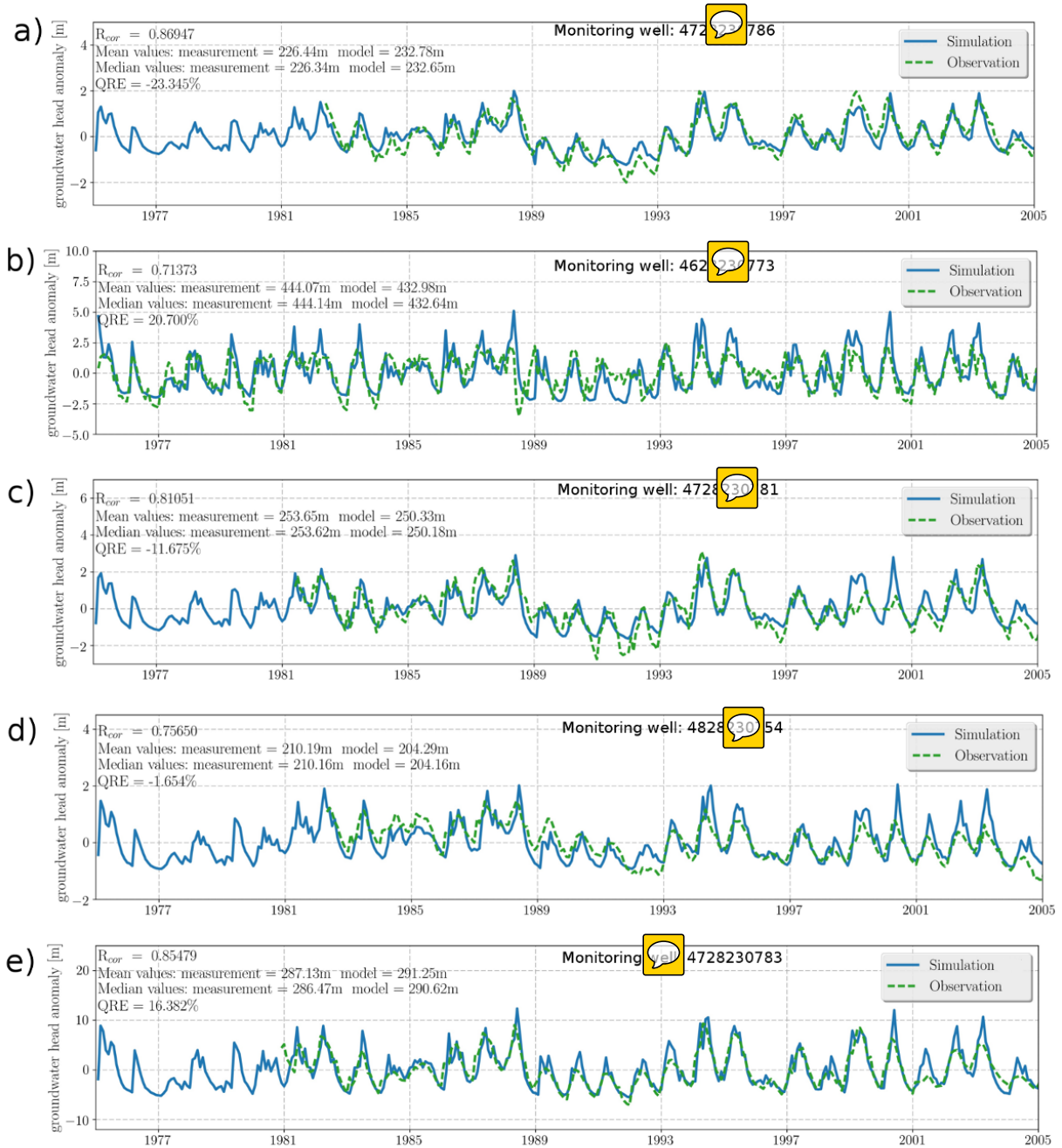
Figure 10. ~~The~~ comparison between measurement ~~data~~ (green dashed line) and ~~model output of~~ groundwater head anomaly (blue solid line). (a) Monitoring well ~~4728230786~~ located at upland near stream. (b) Monitoring well ~~4628230773~~ located at mountainous area. (c) Monitoring well ~~4728230781~~ located at a hillslope at northern upland. (d) Monitoring well ~~4828230754~~ located at lowland. (e) Monitoring well ~~4728230783~~ located at northern mountain.
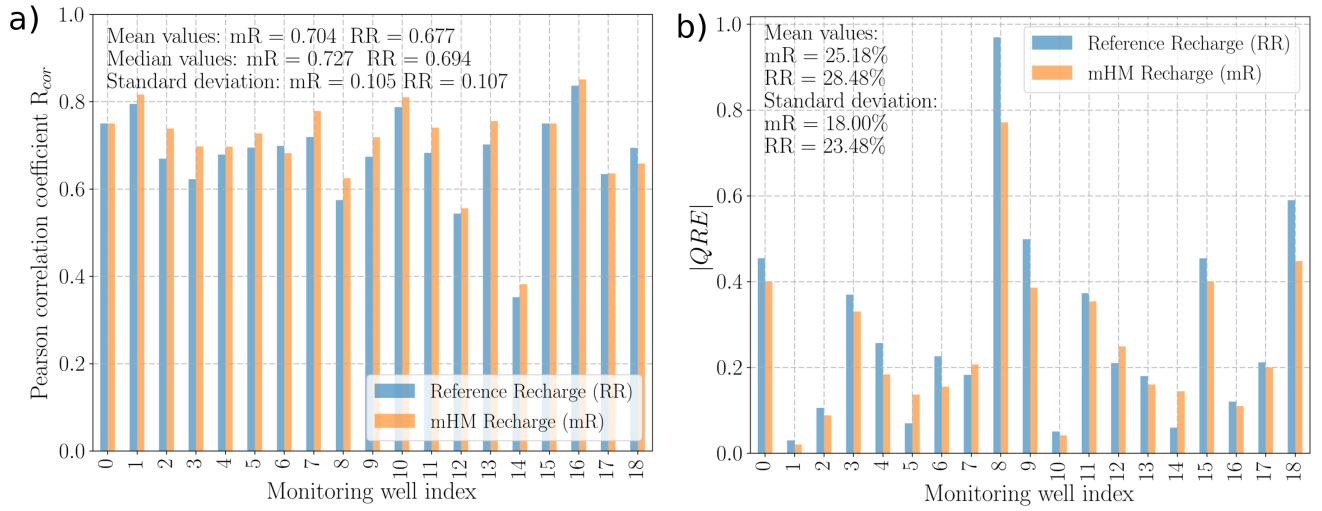
Figure 11. Barplots of a) the Pearson correlation coefficient R_{cor} and b) absolute inter-quantile range error |QRE| in all monitoring wells in two recharge scenarios. Each bar corresponds to an individual monitoring well in the following order: 0 - 4830230779, 1 - 4828230754, 2 - 4828230752, 3 - 4828230753, 4 - 4829230761, 5 - 4829230762, 6 - 4729230719, 7 - 4728230785, 8 - 4728230789, 9 - 4728230788, 10 - 4728230786, 11 - 4728230795, 12 - 4728230797, 13 - 4728230783, 14 - 4728230796, 15 - 4727230764, 16 - 4728230781, 17 - 4628230773, 18 - 4627230764.
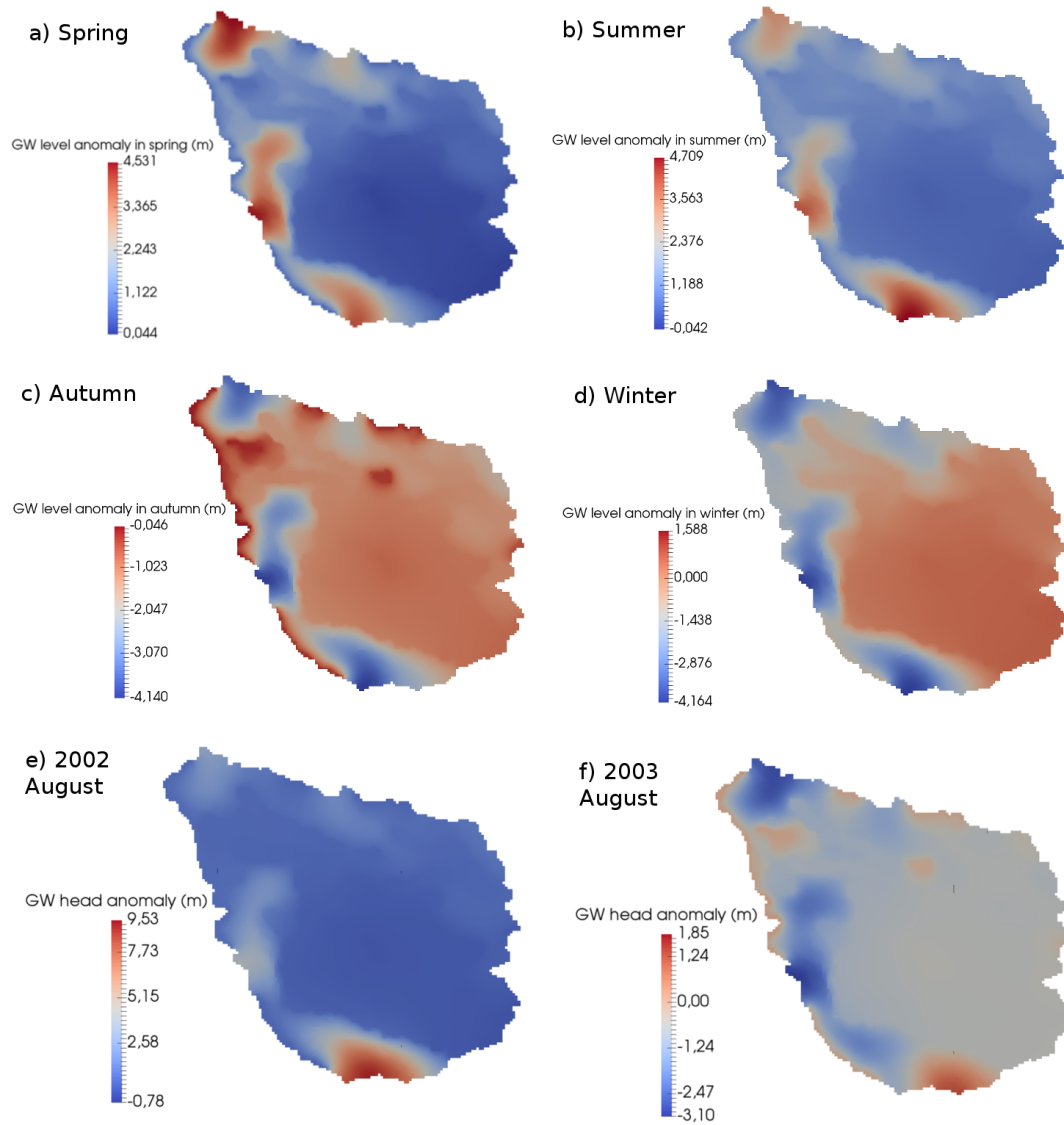
Figure 12. Seasonal variation of spatially-distributed groundwater heads by their anomalies after removing the long-term mean groundwater heads (unit: m). a) Long-term mean groundwater head distribution in spring; b) Long-term mean groundwater head distribution in summer; c) Long-term mean groundwater head distribution in autumn; d) Long-term mean groundwater head distribution in winter; e) Monthly mean groundwater head distribution in wet season (August 2002); f) Monthly mean groundwater head distribution in dry season (August 2003).